Korean J. Chem. Eng., 33(1), 126-131 (2016)
DOI: 10.1007/s11814-015-0117-8

pISSN: 0256-1115
eISSN: 1975-7220

Efficient and selective oxidation of olefins and alcohols using nanoparticles of WO_3-supported manganese oxides ($W_{1-x}Mn_xO_3$)

Mojtaba Amini†

Department of Chemistry, Faculty of Science, University of Maragheh, P. O. Box 55181-83111, Maragheh, Iran
(*Received 3 February 2015 • accepted 30 May 2015*)

Abstract−Nanoparticles of manganese oxide supported on tungsten oxide (WO_3) were synthesized by an impregnation method using $Mn(NO_3)_2$ and Na_2WO_4 as a source of manganese and tungsten. Atomic absorption spectroscopy (AAS), X-ray diffraction (XRD), scanning electron microscopy (SEM) and transmission electron microscopy (TEM) were used to characterize the physicochemical properties of compounds. Due to a highly dispersed state of manganese or insertion of manganese ions into the WO_3 lattice, no manganese oxide peak was observed in the XRD patterns of the $W_{1-x}Mn_xO_3$ nanoparticles. Investigation of $W_{1-x}Mn_xO_3$ by AAS and EDX showed that the relative atomic abundance of Mn present in the bulk and on the surface of WO_3 was 3.68% and 4.8% respectively. For the first time, the catalytic oxidation of olefins and alcohols, in the presence of these materials and hydrogen peroxide (H_2O_2) as a green oxidant at room temperature was studied. The recoverability and catalyst leaching of the $W_{1-x}Mn_xO_3$ nanoparticles in epoxidation of styrene as a model reaction were also investigated.

Keywords: Nanoparticles, Heterogeneous, Oxidation, Olefins and Alcohols

INTRODUCTION

Interest in oxidation of olefins and alcohols has been amplified because epoxides and aldehydes are among the most versatile and tremendously useful intermediates in organic synthesis [1-7]. Due to the strain associated with the three-membered ring, epoxides are spring-loaded for reactions with variety of nucleophiles, leading to a wide range of multi-functional organic compounds [8]. Therefore the synthetic community has been fascinated with prospects of selective synthesis of epoxides by olefin epoxidation [9-11].

Heterogeneous catalytic oxidation has been a promising advanced oxidation method to conversion of olefins to epoxides and alcohols to aldehydes [12,13]. Due to the lower cost, relatively low toxicity and environmentally friendly properties, manganese oxides have been reported to be among the most efficient transition-metal oxide catalysts for catalytic oxidation of organic compounds [14-16]. Recently, considerable efforts have been devoted to the design of efficient oxidation catalysts based on mixtures of two or more metal oxides, because the doping process results in changing the chemistry of the surface of treated solids, brings about some changes in the electronic structure of the doped catalysts and may also affect solid-solid interactions between the oxide catalyst and its support [17,18].

Among all the transition metal oxides, MnO_x-based materials are widely used as catalyst for the oxidation of alcohols [19,20], benzene [21], CO [20], and oxidative dehydrogenation of ethyl-benzene [23], as well as other classes of catalytic oxidation processes [24-26]. In general, MnO_x are compounds with a typical berthollide structure that contain labile lattice oxygen. Catalytic properties of MnO_x-supported catalysts are attributed to the capacity for manganese to form oxides with variable oxidation states (MnO_2, Mn_2O_3, Mn_3O_4, and MnO), and to their oxygen storage capacity in the crystalline lattice [27].

We report here for the first time the use of $W_{1-x}Mn_xO_3$ (x=0.048) as an efficient catalyst for the oxidation of olefins and alcohols using H_2O_2 as a green oxidant.

EXPERIMENTAL

1. Materials

All reagents and solvents were purchased from commercial sources and used without further purification.

2. Characterization

Transmission electron microscopy (TEM) was conducted on carbon-coated copper grids using a FEI Technai G2 F20 Field emission scanning transmission electron microscope (STEM) at 200 kV (point-to-point resolution <0.25 nm, line-to-line resolution <0.10 nm). TEM samples were prepared by placing 2-3 drops of dilute ethanol solutions of the nanomaterials onto carbon coated copper grids. Composition was characterized by energy dispersive spectroscopy (EDS) line scans in STEM mode, and by energy-filtered (EF) imaging spectroscopy (EF-TEM). SEM was by Philips CM120 and LEO 1430VP instruments. The X-ray powder patterns were recorded with a Bruker D8 ADVANCE (Germany) diffractometer (Cu-Kα radiation). Manganese content in the bulk and on the catalyst surface was determined by atomic absorption spectroscopy (AAS) and energy-dispersive X-ray (EDX). AAS was performed on a Varian atomic absorption spectrometer AA 110. Prior to analysis, the oxide (1.0 mg) was added to 1 mL of concentrated nitric acid and H_2O_2, left at room temperature for at least 2 h to

†To whom correspondence should be addressed.
E-mail: mamini@maragheh.ac.ir

ensure that the oxides were completely dissolved. The solution was then diluted to 10.0 mL and analyzed by AAS. The products of oxidation of olefins were determined and analyzed by HP Agilent 6890 gas chromatograph equipped with an HP-5 capillary column (phenyl methyl siloxane 30 m×0.32 mm×0.25 μm) and flame-ionization detector. FT-IR spectrum was obtained by using a Unicam Matson 1000 FT-IR spectrophotometer using KBr disks at room temperature.

3. Synthesis

An aqueous solution (10 mL) of $Na_2WO_4{\cdot}2H_2O$ (0.825 g; 2.5 mmol) was acidified with an HCl solution (6 M), and a white precipitate of $WO_3{\cdot}nH_2O$ was obtained. The solid of $WO_3{\cdot}nH_2O$ was washed with water for several times and dried at 50 °C. WO_3 was prepared by dehydration of $WO_3{\cdot}nH_2O$ at 500 °C for 3 h. MnO_x supported on WO_3 was prepared by an impregnation method using $Mn(NO_3)_2{\cdot}4H_2O$ as a source for Mn. The required amount of $Mn(NO_3)_2{\cdot}4H_2O$, to give 5 wt% Mn loading, was mixed and was pulverized with WO_3. MeOH (20 mL) was added to the mixture of $Mn(NO_3)_2$ and WO_3. This mixture was mechanically stirred to ensure the homogeneous distribution of $Mn(NO_3)_2{\cdot}4H_2O$ over the WO_3 support. After stirring, MeOH was evaporated under vacuum using a rotary evaporator. Dissolution of $Mn(NO_3)_2{\cdot}4H_2O$ and evaporation of MeOH were performed three times to optimize the distribution of $Mn(NO_3)_2{\cdot}4H_2O$. After the third evaporation process, the residual solid was ground and calcined at 500 °C for 4 h. MnO_x was prepared by taking an aqueous solution of $Mn(NO_3)_2{\cdot}4H_2O$ and urea as a fuel in a muffle furnace maintained at 500 °C for 4 h.

4. General Procedures for the Oxidation of Olefins and Alcohols

To a solution of olefins or alcohols (0.5 mmol) and catalyst (10.0 mg) in CH_3CN (1.0 mL) was added H_2O_2 (30% in water) (2.0 mmol) as an oxidant. After stirring at room temperature for 4 h, for the product analysis, the solution was subjected to ether extraction (3× 10 mL), and the extract was also concentrated down to 1.0 mL by distillation in a rotary evaporator at room temperature. Then, a sample (2 μL) was taken from the solution and analyzed by GC. The retention times of the peaks were compared with those of commercial standards, and chlorobenzene was used as an internal standard for GC yield calculation.

RESULTS AND DISCUSSION

1. Catalyst Characterization

The X-ray powder diffraction patterns of WO_3 and $W_{1-x}Mn_xO_3$ (x=0.048) are shown in Fig. 1. The XRD pattern of WO_3 support appears to contain peaks corresponding to lattice reflection planes (001), (020), (200), (120), (111), (201), (220), (221), (400), (40 QUOTE), (421), (40), and (42) as referred in the JC-PDS 01-075-2072 [28]. As shown in Fig. 1, it is difficult to estimate manganese particle phases from the XRD pattern, because the most intense lines of the manganese oxide phases almost coincide with the diffraction lines of the support, but its line intensity increased with the loading of manganese on WO_3, attributed to the formation of crystalline manganese oxide. The absence of the XRD peaks of individual MnO_x is a clear indication that manganese is in a highly dispersed state or that insertion of manganese ions into the WO_3 lattice may occur due to the presence of more surface hydroxyl groups in the WO_3 [29].

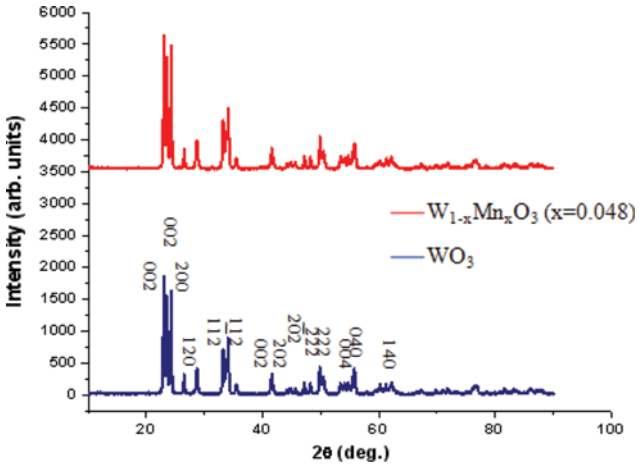

Fig. 1. XRD pattern of WO_3 and $W_{1-x}Mn_xO_3$ (x=0.048).

Table 1. EDX investigation of $W_{1-x}Mn_xO_3$ (x=0.048) catalyst

Element	Weight%	Atomic %	Area scan
O(K)	8.66	49.89	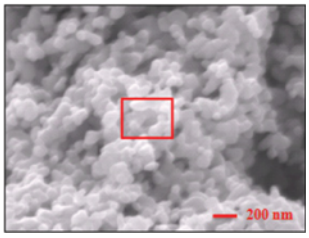
Mn(L)	3.68	6.18	
W(L)	87.65	43.92	

The amount of the manganese on WO_3 was determined by AAS analysis. The catalyst was stirred in HNO_3 at room temperature for 5 h and the solution was subjected to AAS analysis. $W_{1-x}Mn_xO_3$ was contained 4.8 wt% Mn on WO_3. Also, EDX investigation of $W_{1-x}Mn_xO_3$ showed that the relative atomic abundance of manganese present in the surface of WO_3 was obtained 3.68% (Table 1). The differences attained for Mn contents in the bulk and on the surface of catalyst suggest that the composition of the surface layers of the catalyst is slightly different from its bulk composition.

SEM analysis of $W_{1-x}Mn_xO_3$ (x=0.048) catalyst was carried out to find the Mn-distribution on WO_3 (Fig. 2(a)). Aggregated nanoparticles with spherical shapes are observed with a uniform distribution. EDX-Mapping images showed the homogeneous elemental distributions (Fig. 2(b)).

Particle morphology and textural properties of $W_{1-x}Mn_xO_3$ (x= 0.048) catalyst have been also studied carefully by TEM analysis as shown in Fig. 3. $W_{1-x}Mn_xO_3$ (x=0.048) material exhibited spherical-like morphology with particle diameter in the range of 50-80 nm.

2. Catalytic Activity

To check the catalytic activities of $W_{1-x}Mn_xO_3$ (x=0.048) for oxidation reactions, the reactions were optimized according to the oxidation of styrene through the investigation of the influence factors of oxidation, such as the effect of oxidant and H_2O_2/styrene ratio. Various oxidants including TBHP, H_2O_2, NaClO and molecular

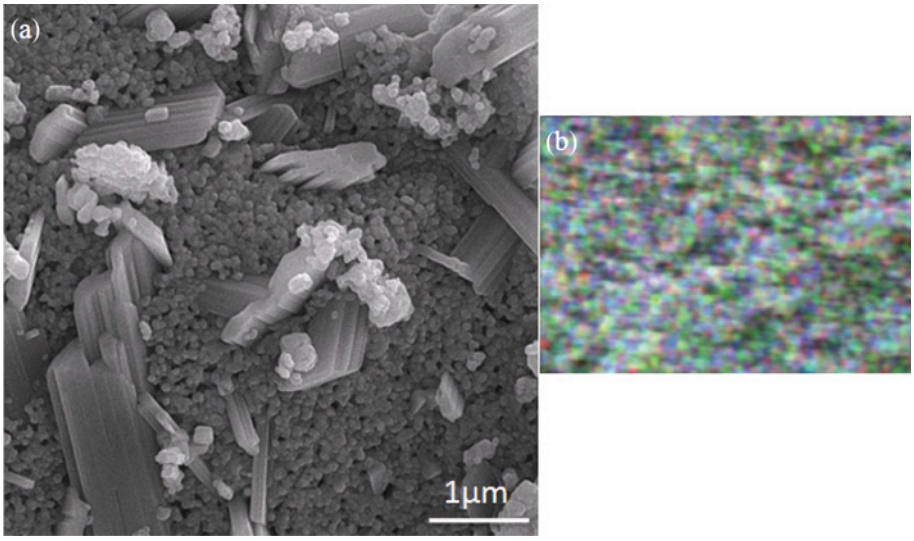

Fig. 2. (a) SEM images of $W_{1-x}Mn_xO_3$ (x=0.048); (b) SEM-EDX images of the $W_{1-x}Mn_xO_3$ (x=0.048) nanoparticles (O: blue; W: green; Mn: red).

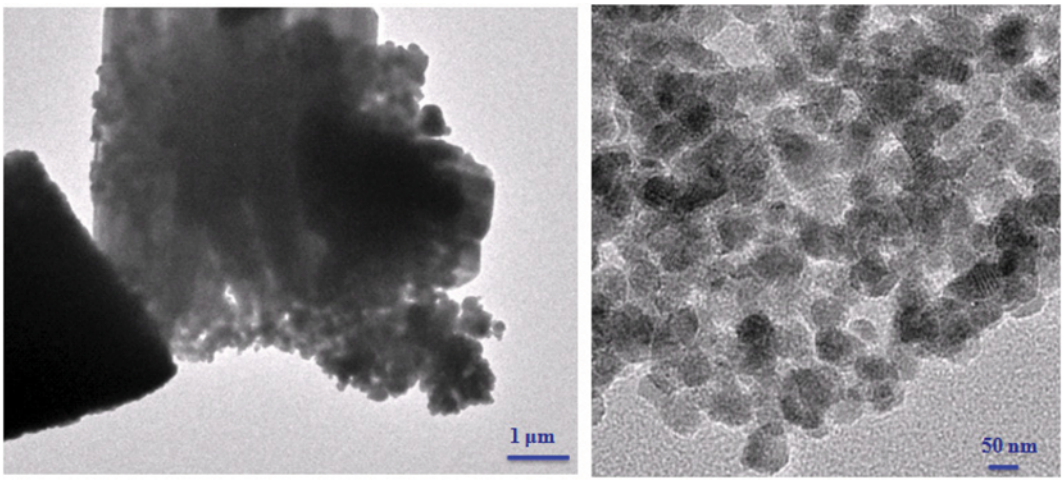

Fig. 3. TEM images of $W_{1-x}Mn_xO_3$ (x=0.048) catalyst.

oxygen were tested for the epoxidation of styrene over $W_{1-x}Mn_xO_3$ (x=0.048) at room temperature. Compared with TBHP, NaClO and molecular oxygen, H_2O_2 was much more efficient for the epoxidation of styrene. The effect of H_2O_2 amount on the styrene epoxidation was studied, which results are shown in Fig. 4. With the H_2O_2/styrene molar ratio varying from 1 to 5, the conversion of styrene quickly increased from 28 to ca. 100%, while the selectivity to styrene oxide remained around 78-99%. When the n(H_2O_2)/n(styrene) was 4, the maximal yield of epoxide was obtained.

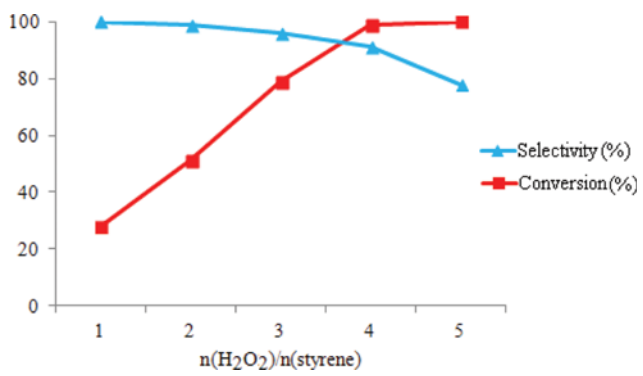

Fig. 4. Effects of H_2O_2/styrene molar ratio on the catalytic performances over $W_{1-x}Mn_xO_3$ (x=0.048) catalyst.

To verify the catalytic scope of the $W_{1-x}Mn_xO_3$ (x=0.048), it has also been applied for the oxidation of a wide variety of alkenes and alcohols (Table 2). When the $W_{1-x}Mn_xO_3$ (x=0.048) catalyst was added to the reaction, the styrene conversion was complete after 4 h. As shown in Table 2, when $W_{1-x}Mn_xO_3$ was replaced by WO_3, the catalytic activity of the system decreased, showing that MnO_x facilitated the oxidation of styrene by H_2O_2. Also, without catalyst a low styrene oxide yield (about 13%) was observed. According to Table 2, it was obvious that $W_{1-x}Mn_xO_3$ could efficiently convert aromatic alkenes (styrene, α-methylstyrene, indene, and 1-phenylcyclohexene) and norbornene to their corresponding epoxides with 93-100% conversion. However, catalytic epoxidation of carbocyclic

Table 2. Epoxidation of olefins catalyzed by $W_{1-x}Mn_xO_3$ (x=0.048) nanoparticles[a]

Entry	Epoxidation reaction[a]	Conversion (%)[b]	Selectivity (%)[c]
1	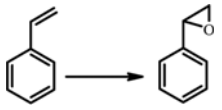	13[d]	100
2	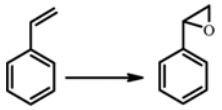	49[e]	98
3	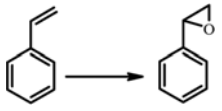	99	91
4	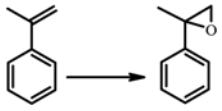	91	95
5	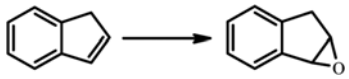	100	98
6	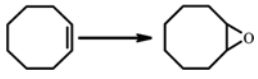	68	89
7	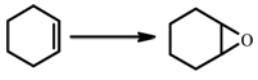	75	83
8	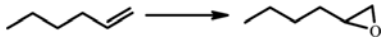	41	100
9		39	100
10	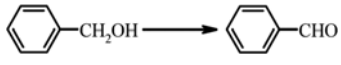	93	75
11	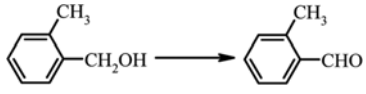	88	81
12	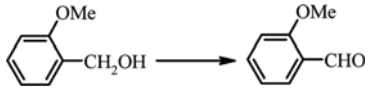	90	81
13	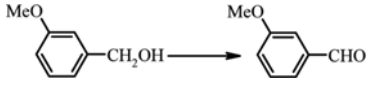	90	83
14		88	80
15	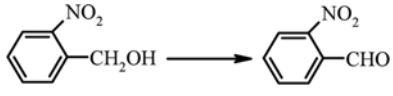	79	97
16	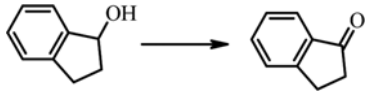	95	100
17	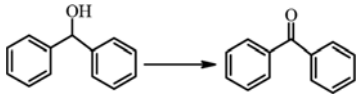	96	100

alkenes like cyclohexene and cyclooctene and the terminal linear alkenes (e.g., 1-hexene and 1-octene) was found to be less efficient. The low π-electron density of linear terminal alkenes decreased the ability of electrophilic cycloaddition within the epoxidation. So terminal alkenes are less reactive toward electrophiles than internal alkenes due to the electron-donating effect to the alkyl substituents. Oxidations of two kinds of secondary alcohols were also investigated and good conversions were obtained. Benzylalcohols

Table 2. Continued

Entry	Epoxidation reaction[a]	Conversion (%)[b]	Selectivity (%)[c]
18	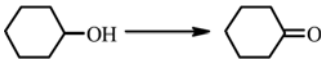	69	100
19	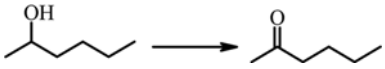	55	100

[a]Reaction conditions: catalyst (10.0 mg), CH_3CN (1 mL), olefins/alcohol (0.5 mmol), H_2O_2 (2 mmol), time=4 h, at room temperature
[b]The GC conversion (%) are measured relative to the starting olefin
[c]Selectivity to epoxide=(epoxide%/(epoxide%+other products%))×100; Selectivity to benzaldehyde=(aldehyde%/(aldehyde%+carboxylic acid%))×100
[d]Reaction in the absence of catalyst
[e]Reaction in the presence of WO_3

were oxidized to the corresponding aldehydes with 79-93% conversions (entries 8-12). The substrates having electron-donating and -withdrawing substituents in the aromatic ring were compatible with this protocol. The change of nature and site of substituents (methyl, methoxy and nitro) in the aromatic ring of benzylalcohol to probe electronic effects displayed almost no regular trends in the conversion. The catalytic oxidation system can over-oxidize aldehyde product to carboxylic acid. Secondary alcohols, e.g., diphenylmethanol and 1-indanole could be converted to the corresponding ketones in 95-96% conversions (entries 14 and 15). Aliphatic alcohols were less reactive in comparison to aromatic alcohols (entry 10). The oxidations of 2-hexanol and cyclohexanol afforded the corresponding ketones with 55% and 69% conversion respectively (entries 16 and 17).

A further set of experiments was performed to check the reusability of the $W_{1-x}Mn_xO_3$ (x=0.048) catalyst for the epoxidation of styrene at room temperature for 4 h, and the results are shown in Fig. 5. For each recycle, the catalyst was recovered from reaction mixture by filtration, washing 2-3 times with distilled water and ethyl ether repeatedly, dried at 50 °C for half an hour, and reused for the next run. The catalyst could be recycled six times with no significant loss in the activity. The conversions of styrene showed a small fluctuation in the range of 87-ca. 99% and the selectivity of epoxide kept around 89-93% during recycling.

By comparing the SEM images of fresh and recycled $W_{1-x}Mn_xO_3$ (x=0.048) catalyst, it was found that catalyst agglomerated seriously after six repeated cycles of the oxidation reaction (Fig. 6(a)). Also the diffraction peaks in the XRD of the used catalyst match very well with monoclinic phase of WO_3 (Fig. 6(b)). However, the particle size calculation based on XRD peak broadening reveals significant metal size growth for the used catalyst. Thus, agglomeration of catalyst can be primarily responsible for the reduction of the $W_{1-x}Mn_xO_3$ (x=0.048) catalytic activity upon its repeated use.

To investigate catalyst leaching in the epoxidation of styrene as a

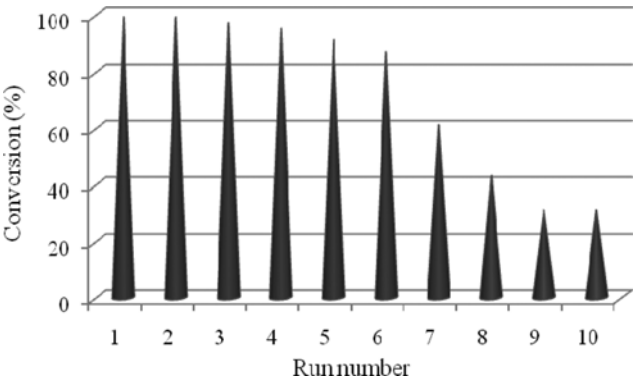

Fig. 5. Recycling studies of the $W_{1-x}Mn_xO_3$ (x=0.048) in the reaction of epoxidation of styrene.

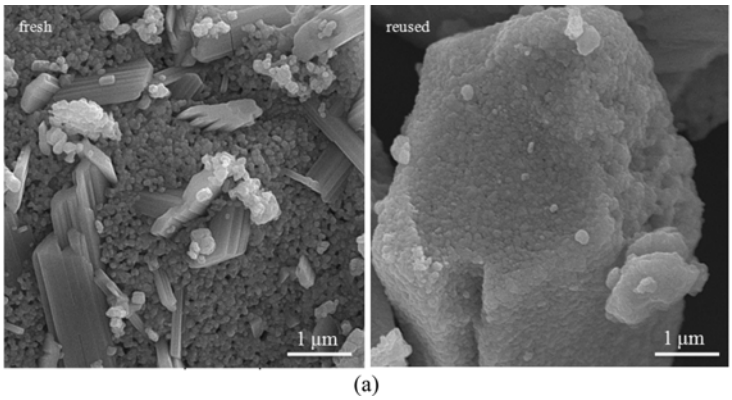

(a)

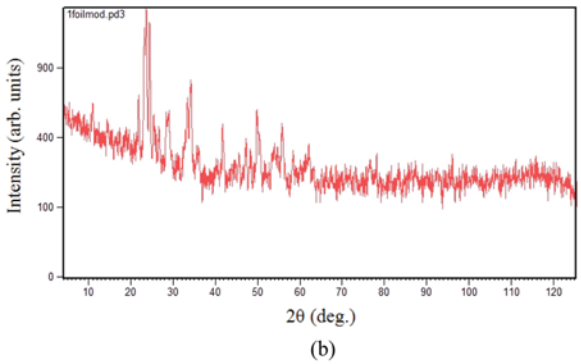

(b)

Fig. 6. (a) SEM images of fresh and reused catalyst, $W_{1-x}Mn_xO_3$ (x=0.048); (b) XRD pattern of reused catalyst.

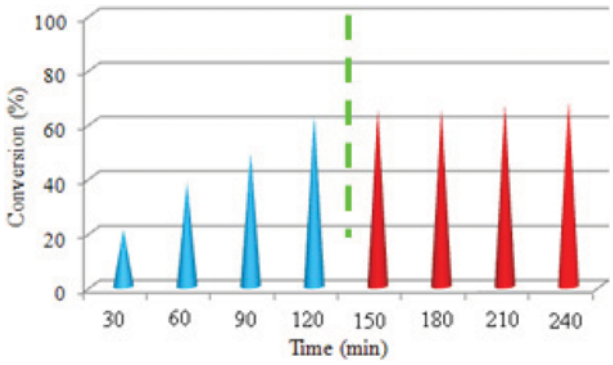

Fig. 7. Leaching experiment; Blue pyramids: reaction with $W_{1-x}Mn_xO_3$ (x=0.048) and red pyramids: reaction without a catalyst.

model reaction, the reaction was stopped at half the reaction time (2 h) and the catalyst was completely separated from solution by filtration. The rest of the reaction mixture (without catalyst) was allowed to stir for another period of half the reaction time. As seen in Fig. 7, a trace amount of styrene oxide was produced after catalyst separation. After separation of the catalyst, the reaction mixture was analyzed by AAS and no manganese was detected. These results show that $W_{1-x}Mn_xO_3$ (x=0.048) is truly heterogeneous and catalyst leaching is negligible under these conditions.

CONCLUSIONS

$W_{1-x}Mn_xO_3$ nanoparticles were synthesized and applied for oxidation of alkenes and alcohols using H_2O_2 as an oxidant in CH_3CN at room temperature. The effects of various oxidants and H_2O_2/styrene ratio as the influence factors of oxidation were also studied. Notably, $W_{1-x}Mn_xO_3$ nanoparticles exhibited the highest activity for the selective oxidation of aromatic alkenes and alcohols with 4 eq. of 30% H_2O_2. With replacement of $W_{1-x}Mn_xO_3$ by WO_3, the catalytic activity of the system decreased, showing that MnO_x facilitated the oxidation of styrene by H_2O_2. The $W_{1-x}Mn_xO_3$ (x=0.048) catalyst could be reused six times without obvious loss in activity and selectivity. Finally, catalyst leaching investigation of $W_{1-x}Mn_xO_3$ (x=0.048) in the epoxidation of styrene as a model reaction showed that catalyst leaching is negligible under reaction condition and the catalytic system is truly heterogeneous.

ACKNOWLEDGEMENTS

M. Amini thanks the Research Council of the University of Maragheh for financial support of this work.

REFERENCES

1. M. Amini, M. M. Haghdoost and M. Bagherzadeh, *Coord. Chem. Rev.*, **268**, 83 (2014).
2. M. Li and Z. Chen, *Res. Chem. Intermed.*, **38**, 1921 (2012).
3. C. Hu, L. Zhang, J. Zhang, L. Cheng, Z. Zhai, J. Chen and W. Hou, *Appl. Surf. Sci.*, **298**, 116 (2014).
4. M. M. Najafpour, M. Amini, D. J. Sedigh, F. Rahimi and M. Bagherzadeh, *RSC Adv.*, **3**, 24069 (2013).
5. A. Askarinejad, M. Bagherzadeh and A. Morsali, *Appl. Surf. Sci.*, **256**, 6678 (2010).
6. M. Lashanizadegan and N. Erfaninia, *Korean J. Chem. Eng.*, **30**, 2007 (2013).
7. Y. S. Ko and W. S. Ahn, *Korean J. Chem. Eng.*, **15**, 182 (1998).
8. X. Lei and N. Chelamalla, *Polyhedron*, **49**, 244 (2013).
9. R. Ghosh, X. Shen, J. C. Villegas, Y. Ding, K. Malinger and S. L. Suib, *J. Phys. Chem. B*, **110**, 7592 (2006).
10. L. Espinal, S. L. Suib and J. F. Rusling, *J. Am. Chem. Soc.*, **126**, 7676 (2004).
11. R. Luo, R. Tan, Z. Peng, W. Zheng, Y. Kong and D. Yin, *J. Catal.*, **287**, 170 (2012).
12. M. R. Maurya, M. Kumar and S. Sikarwar, *Reac. Funct. Polym.*, **66**, 808 (2006).
13. E. Brulé, Y. R. de Miguel and K. K. Hii, *Tetrahedron*, **60**, 5913 (2004).
14. B. Qi, L.-L. Lou, K. Yu, W. Bian and S. Liu, *Catal. Commun.*, **15**, 52 (2011).
15. Q. Tang, S. Hu, Y. Chen, Z. Guo, Y. Hu, Y. Chen and Y. Yang, *Micropor. Mesopor. Mater.*, **132**, 501 (2010).
16. Q. Tang, X. Huang, C. Wu, P. Zhao, Y. Chen and Y. Yang, *J. Mol. Catal. A: Chem.*, **306**, 48 (2009).
17. Y. Peng, Z. Liu, X. Niu, L. Zhou, C. Fu, H. Zhang, J. Li and W. Han, *Catal. Commun.*, **19**, 127 (2012).
18. L. M. Gandìa, M. A. Vicente and A. Gil, *Appl. Catal. B: Environ.*, **38**, 295 (2002).
19. Q. Tang, X. Huang, Y. Chen, T. Liuc and Y. Yang, *J. Mole. Catal. A: Chem.*, **301**, 24 (2009).
20. Q. Tang, X. Gong, P. Zhao, Y. Chen and Y. Yang, *Appl. Catal. A: Gen.*, **389**, 101 (2010).
21. H. Einaga, S. Yamamoto, N. Maeda and Y. Teraoka, *Catal. Today*, **242**, 287 (2015).
22. C. Jones, K. J. Cole, S. H. Taylor, M. J. Crudace and G. J. Hutchings, *J. Mol. Catal., A: Chem.*, **305**, 121 (2009).
23. A. Nishino, *Catal. Today*, **10**, 107 (1991).
24. X. Longya, W. Quigxia, X. Yide and H. Jiashng, *Catal. Lett.*, **31**, 253 (1995).
25. S. Cavallaro, N. Bertuccio, P. Antonucci and N. Giordano, *J. Catal.*, **73**, 337 (1982).
26. F. Kapteijn, D. van Langeveld, J. A. Moulijn, A. Andreini, M. A. Vuurman, A. M. Turek, J. M. Jehng and I. E. Wachs, *J. Catal.*, **150**, 94 (1994).
27. R. Craciun, B. Nentwick, K. Hadjiivanov and H. Knözinger, *Appl. Catal. A: Gen.*, **243**, 67 (2003).
28. A. Hemati, M. Allaf B, M. Ranjbar, P. Kameli and H. Salamati, *Sol. Energy Mater. Sol. Cells*, **108**, 105 (2013).
29. S. M. Kanan, Z. Lu, J. K. Cox, G. Bernhardt and C. P. Tripp, *Langmuir*, **18**, 1707 (2002).